INTERNAL DAMPING OF METAL MATRIX COMPOSITES: A TECHNICAL ASSESSMENT

Jacques E. Schoutens
MMCIAC
Kaman Sciences Corporation

ABSTRACT

Internal damping in metal matrix composites (MMC) is of interest to engineers and designers of large space structures, in applications where dynamic dimensional stability is important, and in the control and damping of vibrations in space structures. Theories of current interest used to understand and explain internal damping in MMCs are discussed briefly, and experimental data for some fibers and MMC systems are presented. Some general conclusions close this paper.

INTRODUCTION

Damping of structures has two sources: external and internal. External sources of damping include the effects of fluids such as drag in a liquid or in a gas, loss of energy at supports or joints due to friction or transmission into supporting structures, and active and passive damping control systems. Internal sources of damping include a number of effects. At low levels of stress, the damping behavior of metals and metal matrix composites is governed by micromechanisms causing anelastic behavior. At high levels of stress [1,2] internal damping occurs by mechanisms leading to hysteretic response. Internal damping in metals has been used as a method of studying atomic motion at low stress levels. This has provided insight into fundamental mechanisms in diffusion, ordering, interstitial and substitutional solid solutions, and estimates of dislocation densities. For engineering applications, damping data have been obtained at intermediate and high strain levels ($>$ 50 microstrain) to develop insight into energy dissipation mechanisms and fatigue life of metal components. As is well-known, the interface between a fiber and the matrix is a unique site of reaction layers, residual stresses, microvoids, dislocation structures, impurities, disbonds, and other defects. It has been postulated, and to some extent verified, that the interface is also a source of energy dissipation, and considerable efforts have been expended in attempting to identify and model these sources [3]. It should be borne in mind that selecting materials for effective damping must take account of the space environment (zero gravity, high vacuum, and thermal fluctuations between -160 to +160°C), and candidate materials must exhibit high damping at low frequencies (0.1 to 10 Hz) [2] and at strain levels on the order of 50 microstrain.

This paper presents a brief discussion of currently used theories of internal damping in MMCs, and presents some of the available data on internal damping of these advanced materials. For more details, the reader is referred to reference 4 or 5.

---

816 State Street, P.O. Box 1479, Santa Barbara, CA 93102-1479, (805)963-6426.

THEORY

The methods for measuring damping in metals and metal matrix composites span some seventeen orders of magnitudes in frequency, from about 10^{-6} Hz to 100 GHz. There are four major categories covering this range: quasi-static methods, subresonance methods, resonance methods, and high-frequency wave propagation methods [5]. The quasi-static method is of no interest in this paper, and the high-frequency range will not be discussed because it is used mainly to measure dynamic moduli and other phenomena [8].

The damping properties of a material are variously referred to as specific damping capacity, loss factor, loss angle, quality factor, and log decrement. These quantities are all related as follows [4,5]

$$\Psi = 4\pi\xi = 2\pi Q^{-1} = 2\pi\eta = 2\pi\tan\phi = 2\zeta \qquad (1)$$

where Ψ is the specific damping capacity (SDC), ξ is the damping ratio, Q is the quality factor, η is the loss factor, ϕ is the loss angle and ζ is the logarithmic decrement. Most of the data presented in this paper will be in terms of the specific damping capacity.

The methods used to measure damping properties are discussed in detail in reference 4. Suffice it here to mention that they include the cantilever beam method, free-free flexure method, tension-tension method, free fall method, piezoelectric ultrasonic composite oscillator technique (PUCOT) [5], and the method of wave propagation. These methods give slightly different results; consequently, data must be corrected accordingly [4,5]. Damping factors are measured as a function of strain amplitude, temperature or frequency.

The following summarizes the various damping mechanisms and the theories used to explain these mechanisms. Note that some theories predict certain behavior fairly well in a particular range of interest, but by and large, theoretical models used to predict damping behavior are rather primitive, particularly for MMCs. Little or no theoretical work has been done for the fiber/matrix interface.

Matrix Metal. Damping in the matrix metal can occur from any one or all of the following mechanisms: point defect damping, dislocation damping, grain boundary damping, and thermoelastic damping.

A point defect in a crystal can be a vacancy or extra atom either in the crystal lattice or as an impurity atom. This alters the crystal, thereby lowering the crystal symmetry, termed a defect symmetry. The criterion for the existence of point defect damping is that there must be more than one distinguishable orientation of the defect. The elastic distortion surrounding the defect causes the point defect to interact with the crystal lattice, behaving as an elastic dipole. Different defects will interact differently causing some redistribution of the orientation of the point defects. It is this redistribution that is the damping mechanism. For metals with cubic crystal lattice, the following types of defects having non-symmetrical strain fields give rise to

damping [5]: interstitial impurities, vacancy-impurity pairs, and divacancies. Spherically symmetric strain fields do not cause damping. The first of these defects give rise to Snoek relaxation, and the second to Zener relaxation. Snoek relaxation is expected to contribute to damping in MMCs with bcc crystal lattices, and Zener relaxation contributes to internal friction in alloys [4,5] of fcc, bcc, and hcp structure.

Dislocation damping plays an important role in crystalline MMCs. This damping mechanism involves the motion of dislocations which lag behind the applied stress. In some metals (Cu for example) the application of stress will also cause the generation or multiplication of dislocations. Damping occurs when dislocations are hindered in their motion by obstacles such as point defects. There are two relevant mechanisms in MMCs; relaxation or resonance absorption (Zener), and hysteresis losses. Granato and Lucke [4,5,7] developed a model for dislocation damping that is based on the vibrating string model, where the string is the dislocation motion while pinned at both ends by defects. This is an important model because it has been used to calculate mobile dislocation densities and the spacing between impurity atoms on dislocation lines from measurements of strain amplitude dependent damping [5].

Zener [6] predicted that grain-boundary relaxation occurs by viscous sliding between adjacent grains. Nowick and Berry [7] show that the viscous slip model predicts a relaxation that is essentially independent of grain size, as long as the grain size is less than the specimen diameter. A satisfactory quantitative theory of grain-boundary relaxation is not yet available [5].

Thermoelastic damping is the result of coupling between the conjugate pair stress and strain, and the conjugate pair temperature and entropy, as for example during expansion where the specimen length can be changed by stretching or by heating. This means that a change in entropy with respect to stress (T=const.) is equal to the change in strain with respect to temperature (constant stress), and is identical to the coefficient of thermal expansion [5]. When a beam, plate, or rod vibrates, relaxation takes place under inhomogeneous stress. Bending of isotropic materials induces uniaxial strain which varies linearly with distance from the neutral axis. As the beam vibrates, an alternating temperature gradient is set up across the beam, and relaxation occurs by heating and heat transfer across the specimen. In the case of longitudinal thermal currents induced by vibrations, Nowick and Berry [7] showed that this kind of damping is negligibly small at frequencies below 100 MHz.

Fiber. Only limited experimental results and theoretical modeling have been reported. The fiber is usually assumed to be a perfectly elastic material contributing little or no damping to MMCs [9]. Internal damping in boron fibers and whiskers was studied experimentally and theoretically using torsional oscillations [10-12]; Postnikov et al [13] using bending oscillations in the kHz range studied the internal friction in boron fibers. These researchers obtained dynamic modulus data as a function of temperature. Internal friction in boron fibers is characterized by a peak between 530 and 630°C. Models published so far treat continuous fibers as a single material, which clearly is not correct. Continuous fibers are built up on a substrate of either tungsten or carbon; the outer surface of the fiber is coated, sometimes with an elastically compliant coating and/or a reaction barrier.

Fiber/Matrix Interface Damping. The presence of an interface and/or a reaction layer between fiber and matrix raises the possibility of introducing a controlled source of damping in metal matrix composites. Modeling of the effects of damping on MMCs by Nelson and Hancock [15] predicted the interface friction slip. Their model consisted of a frictional energy loss at the interface and viscoelastic energy dissipation in the matrix when the composite is subjected to cyclic tensile loading. Good agreement with experiment was noted for a model consisting of discontinuous, aligned fibers, loaded along the fiber direction. Transverse loading of a linearly elastic material with rigid cylindrical reinforcement was modeled by Kishore et al. [16,17], in which no slip, slip, and interface separation could be introduced; only frictional losses were considered. The loss factor, not surprisingly, was found to depend on fiber volume fraction, coefficient of friction at the interface, load amplitude and constraint stresses at the interface. Whisker or particulate reinforced matrix may exhibit increased specific damping capasity due to stress concentrations near the ends of the reinforcement; stress concentration results in increased dislocation density. Ledbetter and Datta [18] modeled the internal friction for scattering of stress waves by elastic particles dispersed in the matrix, and predicted an increase in friction with increasing particle concentration, increase in particle characteristic length, reduction in aspect ratio, and increases in the difference between particle and elastic stiffness. A more recent model proposed by Ledbetter et al [8] suggested an approach followed up by Schoutens [14] with a simple model based on the thickness of the reaction layer. No results were obtained because of the difficulty in assigning some damping properties and friction coefficients for the reaction layer. Modeling of damping caused by the presence of discontinuous fiber reinforcement in a metal matrix indicates that damping is increased by an increase in the fiber-end gap dimension, for a given fiber volume fraction, and a decreasing fiber aspect ratio [19]. Differences in the coefficient of thermal expansion between reinforcement and matrix produces residual stresses which produce dislocation substructure. Damping increases with increasing dislocation density. The amount of damping produced by these dislocations can be calculated with the Granato-Lucke theory [4]. The role of residual stresses at the interface has been verified by experiments [2]. These test results show that stress-relieved and T6 stress-relieved P55/6061 Al specimens exhibit lower specific damping capacity than the as-fabricated specimens. However, heat treatment is in the primary recrystallization range, and recrystallization is known to reduce damping by decreasing the dislocation density in the matrix, and by increasing the size of grains. Stress-relieved specimens showed nearly strain-amplitude-inpendent damping response even at intermediate strain amplitudes, while as-fabricated specimens showed strain-amplitude-dependent behavior. When stress-relieved specimens were reheated to 540°C (close to the consolidation temperature) and slowly cooled to room temperature, measurements showed damping values consistent with as-fabricated specimens.

Combined Mechanisms. In the absence of detailed theories to predict the specific damping capacity of MMCs, it is tempting to use the rule of mixtures to predict properties from those of the constituents. In this way, the specific damping capacity is predicted from the sum of specific damping capacity of constituents weighed by their fraction in the composite. The fraction of damping due to the interface reaction layer is also included in this sum. The matrix damping, is the sum of contributions from dislocations, point defects, grain boundaries and other relevant effects. This approach generally over simplifies the problem considerably, and in consequence cannot be considered as reliable. Hashin [20] showed how the correspondence principle may be used to relate the effective viscoelastic functions for composites to the effective

moduli. This method has resulted in reasonably good predictions of specific damping of MMCs [5].

For many MMCs, one or two damping mechanisms usually dominate for a given combination of strain amplitude, temperature and frequency. Predictions from dislocation damping (Granato-Lucke model) and thermoelastic damping (Zener relaxation) have turned out to be useful. For predicting damping from constituent properties, Hashin's correspondence principle has been useful [5].

INTERNAL DAMPING DATA

Internal damping data has been reported most often as specific damping capacity Ψ (SDC) in percent, and less often as the loss or quality factor. Damping is generally shown as a function of strain amplitude, frequency, or temperature. For example in pure aluminum, the damping capacity shows very little dependence on strain amplitude until the strain amplitude reaches approximately 10^{-4}, and beyond this point the damping capacity rises fairly steeply. Damping capacity, as we will show, varies also as function of frequency. The damping capacity also rises with increasing temperature, sometimes exhibiting a maximum. Table 1 presents the damping capacity of unreinforced structural materials. MMCs have a damping capacity in the 0.1% to 30% range at frequencies ranging from approximately 1 Hz to a few kHz.

Table 1 - Specific Damping Capacity (Ψ) for Some Unreinforced Structural Materials

Material	Ψ(%)	Frequency Range
403 SS Nivco NiTi Cast iron Cast Pure Mg	6-40	kHz
2024 T3 6061 T6 1020 Steel	0.4-3	Hz-kHz
310 SS Ti-6Al-4V	0.1 - 0.2	40 kHz
Brass	~0.06	kHz
MMCs	~0.1 - 30	Hz-kHz

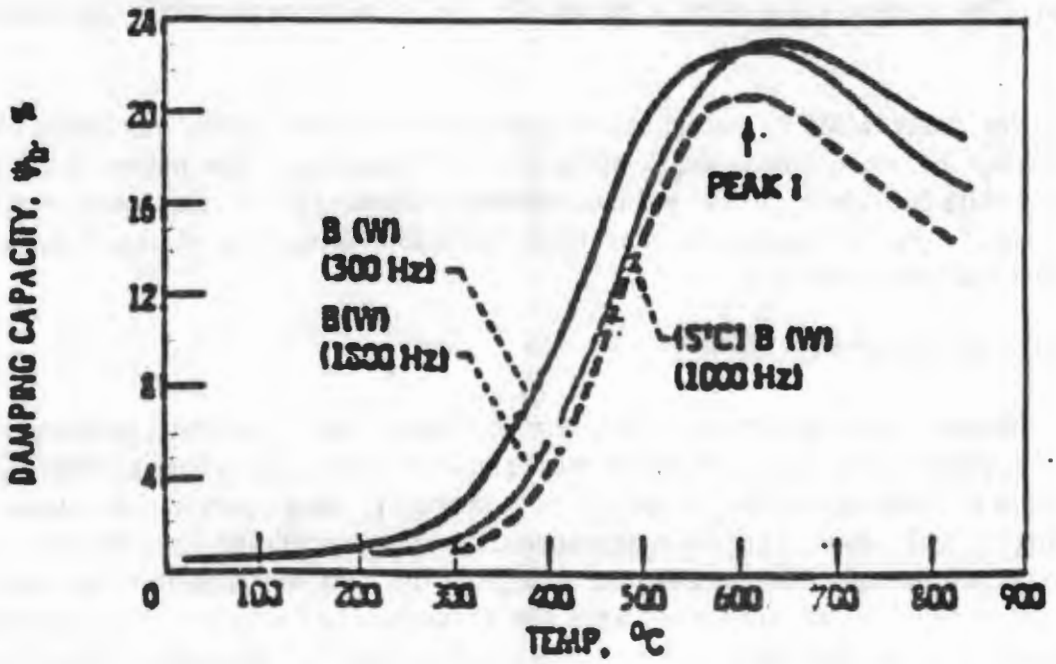

Figure 1 Damping Capacity of boron fiber and silicon carbide coated boron fibers [9]

Figure 1 shows the damping capacity of boron fiber and of silicon-carbide-coated boron fibers, as a function of temperature. Both filaments were produced on a tungsten core. The data were obtained at 300 and 1800 Hz for the boron fiber and at 1000 Hz for the SiC-coated boron fiber (Borsic). DiCarlo and Williams [9] noted that the damping capacity decreased with heat treatment cycles. The damping agrees with measurements on boron fibers made in the Soviet Union [10-13]. Borsic exhibits a consistently lower damping capacity over most of the temperature range of interest, compared to uncoated boron fibers. At 600°C, the damping of both fibers is approximately a factor of 20-23 higher than at room temperature. The prediction of the maximum damping capacity made by Postnikov et al. [13] is approximately a factor of 10 below measured values.

Figure 2 shows the damping capacity of silicon carbide fiber as a function of frequency, and Figure 3 shows the damping capacity of the same fiber as function of temperature. In Figure 3 we see a sharp rise in the damping capacity with a rise in temperature. Figure 2 shows that there is a significant effect on the damping capacity of the fiber due to thermoelastic effects. This effect rises above the damping capacity due to the microstructure. The peak damping capacity is at about 2500 Hz, where it has increased by a factor of about four above that of due to the microstructure. The curve seems to be fairly broad, ranging from approximately 200 Hz to 50 kHz. A similar but broader peak as a function of temperature has been reported for bromide treated pitch-base carbon fibers [21]. SiC fiber damping capacity is considerably lower than for boron fiber, by a factor of 10-12.

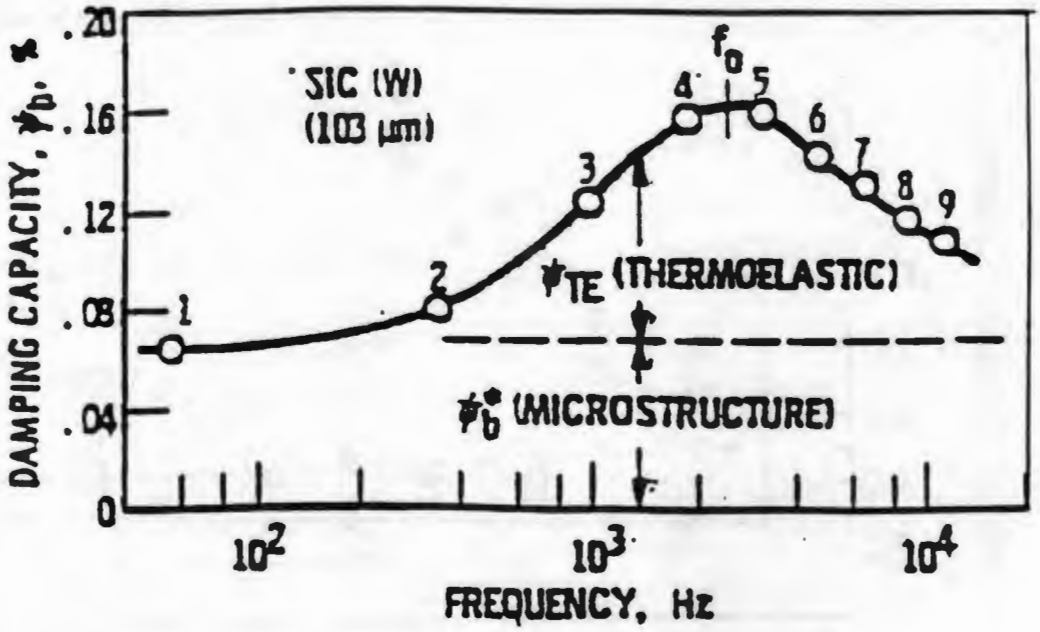

Figure 2 Damping capacity of SiC fiber at 26°C for the first nine flexural tones. Fiber diameter 103 μm. Core: tungsten [9].

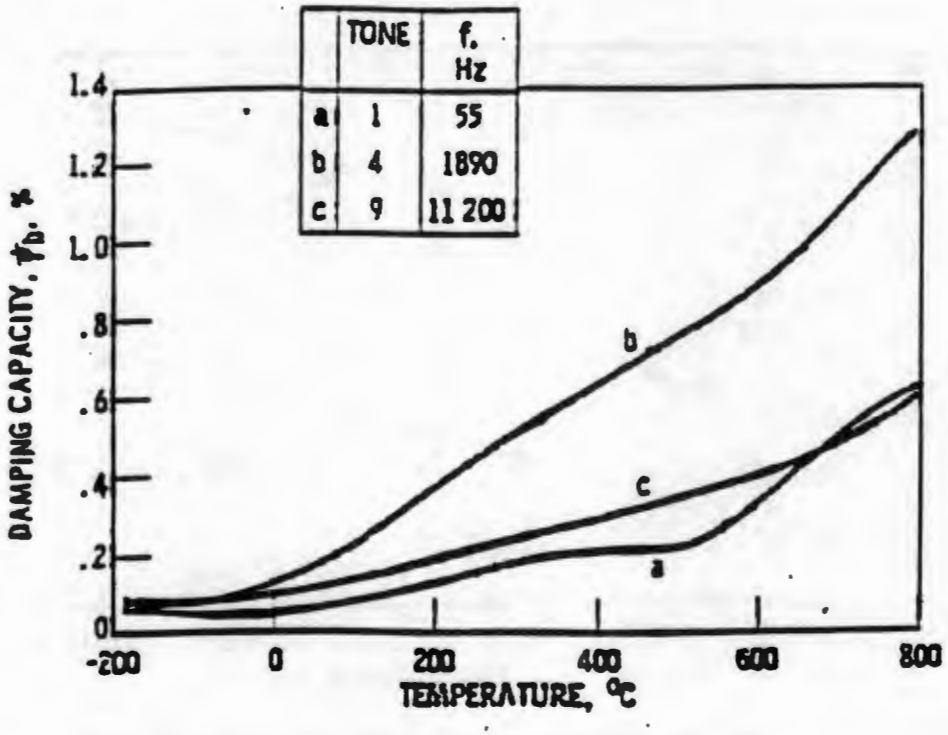

Figure 3 Damping capacity of SiC fiber at three flexural tones. Fiber diameter is 103 μm. Core: tungsten [9].

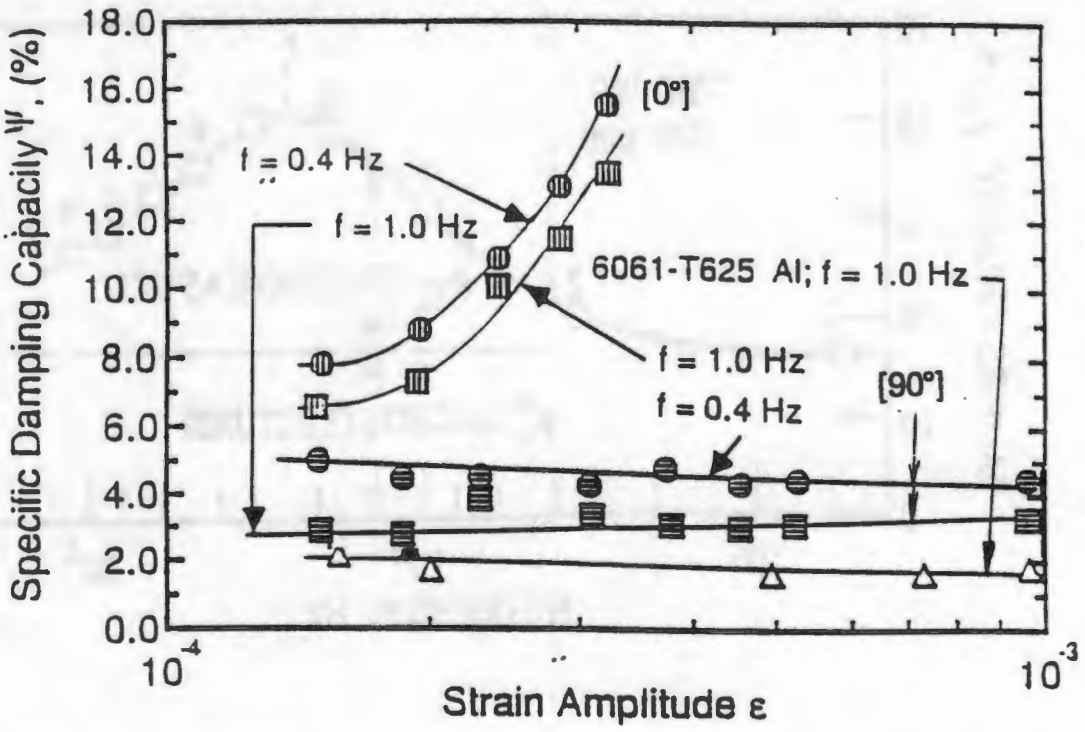

Figure 4 Damping capacity of P55Gr/6061 Al composites for [0°] and [90°] fiber orientation [2]. (Tension-Tension Fatigue Test)

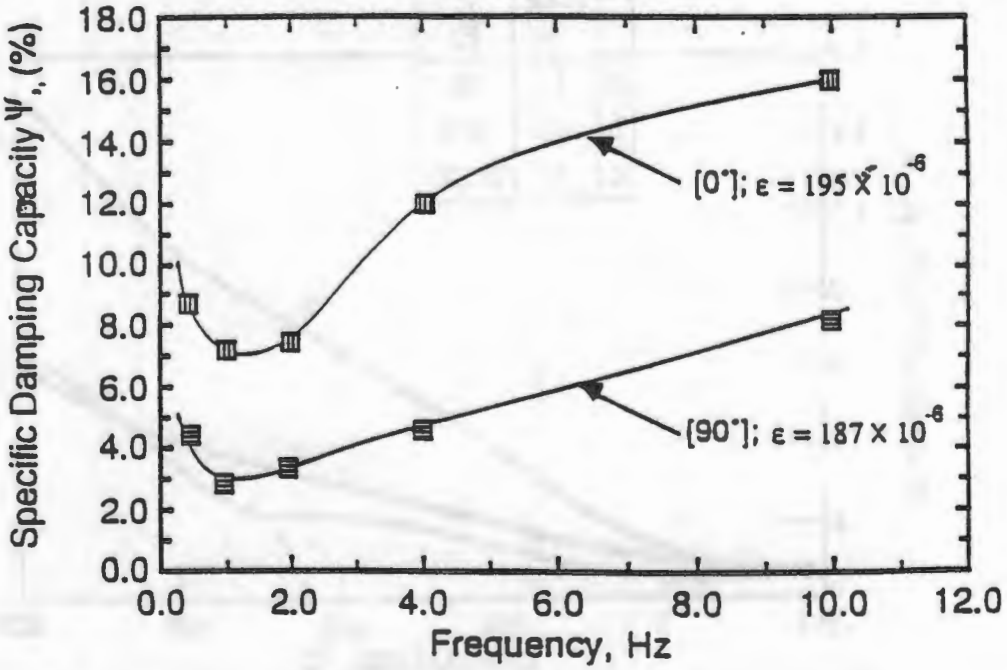

Figure 5 Damping capacity of P55Gr/6061 Al as a function frequency for [0°] and [90°] fiber orientation. (Tension-Tension Fatigue Test) [2].

Figure 4 shows the damping capacity of P55/6061 aluminum composite as a function of strain amplitude and for two ply orientations. Measurements were performed in a tension-tension fatigue test. These data were obtained at frequencies of 1 Hz and 0.4 Hz. This frequency range also corresponds to a frequency range where the damping capacity is a minimum. Note that the [0°] orientation gives a fairly fast rising damping capacity with only modest increases in strain amplitude. Conversely, the [90°] orientation remains fairly constant with strain amplitude.

Figure 5 shows the damping capacity of P55Gr/6061 aluminum as a function of frequency for two ply orientations, [0°] and [90°]; the data were obtained from tension-tension fatigue tests at approximately 190 microstrain. Note the minima in these curves at approximately 1 Hz, and the fact that the longitudinal data ([0°]) exhibits a higher damping capacity than the transverse data ([90°]) by about a factor of two.

Figure 6 shows the damping capacity of P55Gr/Mg - 0.6 at. % Zr as a function of temperature. The material was tested in the as-cast condition, and the result of several indicated heat treatments are shown. The measurements were made at 0.1 microstrain. The damping capacity exhibits a peak at approximately 200°K, and a minimum at about 300-400°K. As indicated, this peak has been attributed by Misra and co-workers [22] to a phase transition in the graphite fibers from a rhombohedral phase to a hexagonal close-packed phase. The difference in the damping capacity between the maximum and minimum values is approximately 36%. Overall the damping capacity of this kind of graphite/magnesium composite is not very high, only 0.8-0.9%.

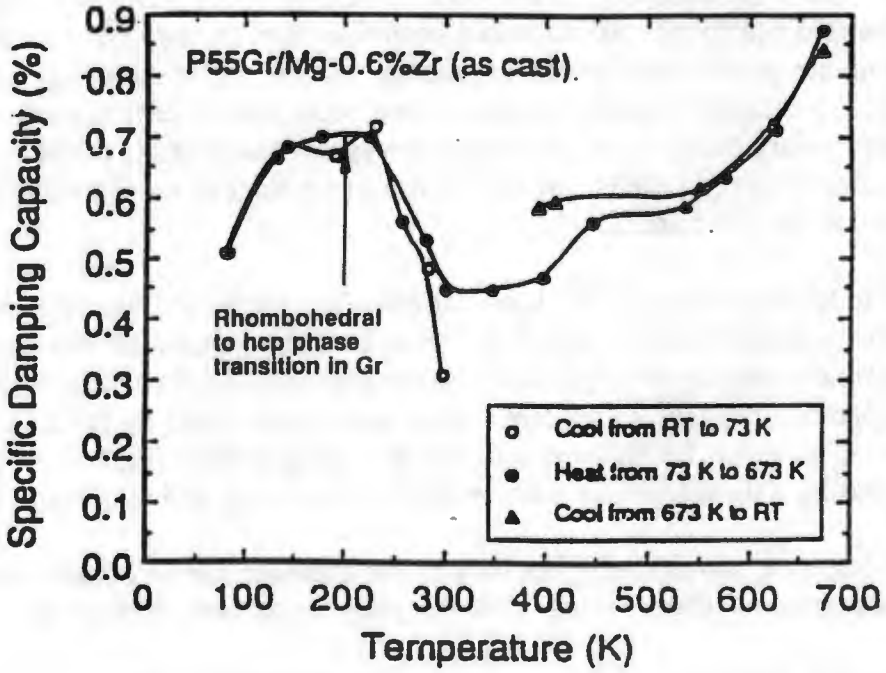

Figure 6 Damping capacity of as-cast Gr/Mg-0.6 at. % Zr as a function of temperature [22].

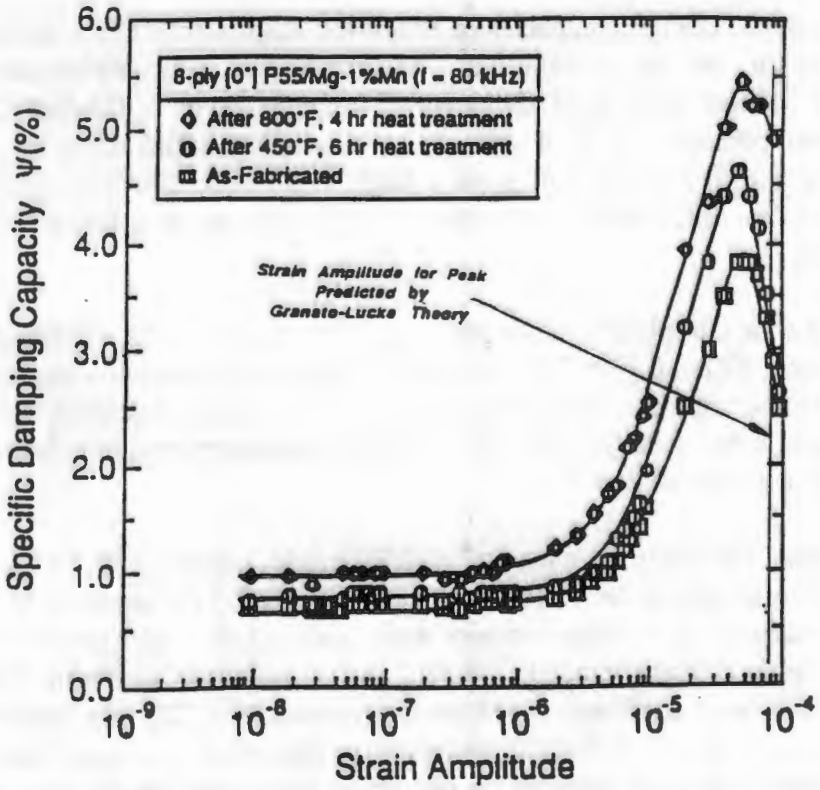

Figure 7 Damping capacity of P55Gr/Mg-1 at.% Mn as a function of strain amplitude [22].

Figure 7 shows the damping capacity of P55Gr/Mg - 1 at.% Mn as a function of strain amplitude. The data are for the as-fabricated condition, and for two types of heat treatment. Unlike the aluminum matrix, heat treatment causes a modest rise in damping capacity. For all three conditions the damping capacity increases from about one percent to about five percent at strain amplitudes greater than 2×10^{-6}, and decreases again following the peaks at about 5×10^{-5}. The Granato-Lucke theory was used to predict the strain amplitude at which the damping capacities are a maximum: at 80 microstrain.

The axial damping capacity of silicon-carbide-fiber-reinforced titanium for the indicated values of the fiber volume fraction is shown in Figure 8. The vertical scale was expanded relative to the horizontal scale, creating the impression that the damping capacity undergoes large variations with small temperature changes. Predicted values based on a model by DiCarlo et al. [23] are plotted on the bottom graph for frequency values of 1200 and 2000 Hz. These predictions are quite low, increasing only marginally with increasing frequency and temperature.

These computed curves testify not only to the inadequacies of current models, but also to our lack of fundamental understanding of the damping mechanisms in metal matrix composites.

The damping properties of SiC particulate- and whisker-reinforced aluminum material are shown in Tables 2 and 3. The damping capacity and the frequency at which these data were obtained are shown at the extreme right in these tables. For constant fiber volume concentration, both SiC particulate- and whisker-reinforced aluminum exhibit damping capacity

Table 2 Specific damping capacity of SiC_p/Al and SiC_wAl [24].

Fiber	Matrix	Fiber Vol. (%)	Elastic Mod. (msi)		Density (g/cm^3)	Freq. (Hz)	Ψ (%)
			Trans.	Long.			
SiC_p	CT90 Al	20	17.1	17.1	2.962	62.25	3.98
SiC_p	CT90 Al	20	17.8	17.8	2.962	111.00	3.20
SiC_w	2024 Al	20	15.4	15.4	2.962	53.25	4.72
Sic_w	2024 Al	20	16.3	16.3	2.962	110.00	3.05

Table 3 Specific damping capisity for SiC_p/6061 and SiC_w/6061 composites [25].

Material	Fiber Vol. (%)	Elastic Mod. (msi)	Ultimate Strength (ksi)	Elonga-tion to Failure (%)	Freq. (Hz)	Ψ (%)
SiC_w/6061-T6(L)*	17	14.7	73	2.1	32.1	1.571
SiC_p/6061-T6(L)*	20	15.2	70	4.5	120.0	2.890
SiC_p/6061-T6(L)*	30	17.5	77	3.0	20.1 104.7	2.325 0.817
SiC_p/6061-T6(T)**	30	17.5	77	3.0	105.4	0.942

* Extended and cross-rolled sheet, L = longitudinal to the extension direction. The mechanical properties for the 20 v/o SiC_p/6061 composites are those for the T6 condition. However, the damping measurements are given for the composites in the F condition.

** Rolled sheet.

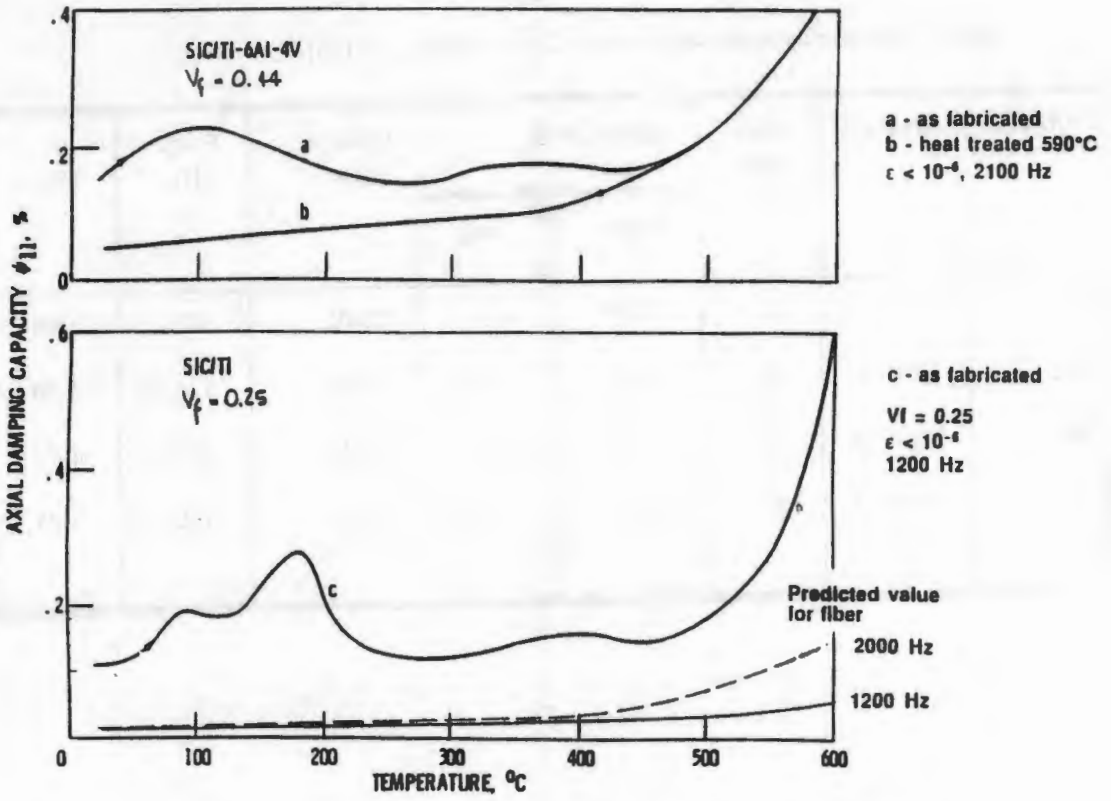

Figure 8 Axial damping capacity of SiC fiber reinforced Ti-6Al-4V [23].

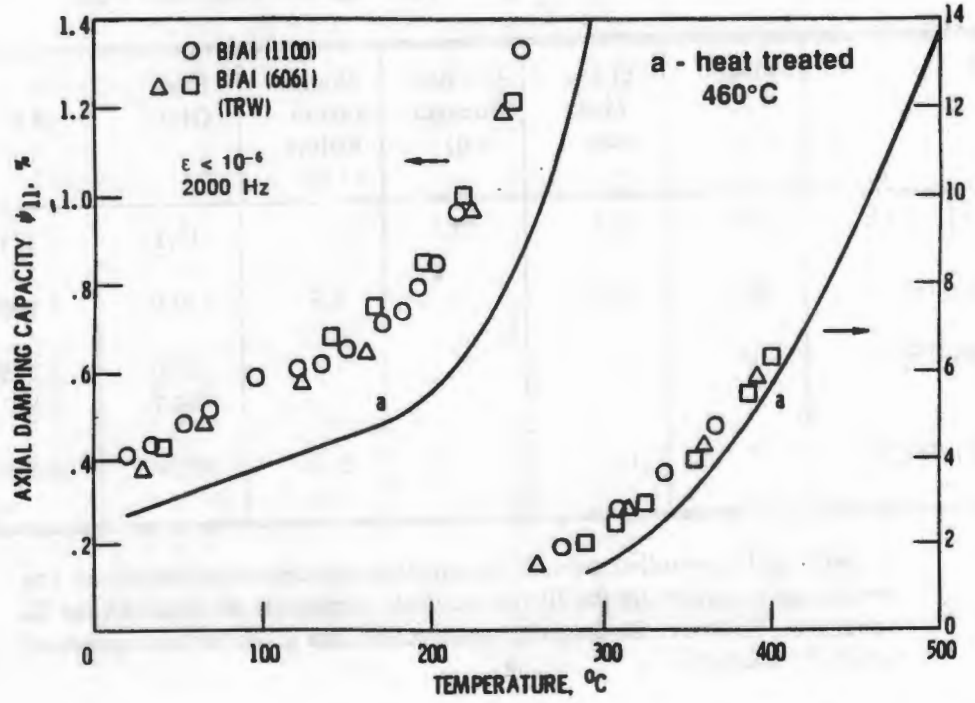

Figure 9 Axial Damping Capacity of B/1100 Al and B/6061 Al [23].

of about 3 to 5 percent which does not appear to depend on matrix type. Table 3 shows a significant reduction in damping capacity due to a change in the orientation of the specimens. These variations taken collectively may be due to process variations, reinforcement concentration, and testing frequency.

Figure 9 presents axial damping capacity of B/1100 Al and B/6061 Al. Two scales are used to show the large change in Ψ with temperature. These measurements were made at less than one microstrain and at 2000 Hz. The B/6061 Al material was fabricated by TRW, Inc. The solid curve represents the same material after subjecting it to a heat treatment at 460°C. The heat treatment is in the primary recrystallization range of aluminum. Recrystallization is known to reduce damping (by decreasing the dislocation density in the matrix), and to increase the matrix grain size. No systematic studies of the effects of heat treatment on boron/aluminum materials seem to have been carried out.

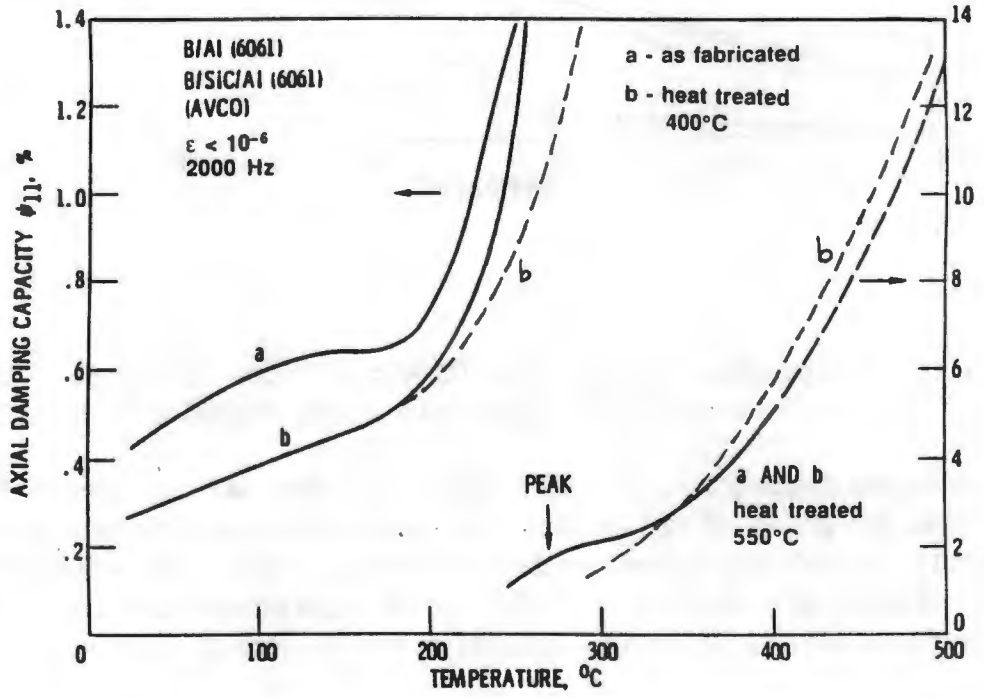

Figure 10 Axial Damping Capacity of B/6061 Al and Borsic/6061 Al [23].

The effects of a SiC coating on boron fiber (Borsic) used in reinforcing 6061 Al is shown in Figure 10. This material was fabricated by Avco, now H.R. Textron. Note that the heat treatments reduce the damping capacity of the composite: this is caused by a reduction in dislocations in the matrix near each fiber by grain growth due to recrystallization. The dashed curves labeled c are the curves labeled a in Figure 9. The other dashed curve on the left and curve c are for damping of Borsic/6061 Al specimens after heat treatment to 550 °C. These data were obtained at 2000 Hz and 1 microstrain [4,23]. The duration and cooling mode of these specimens were not reported [5].

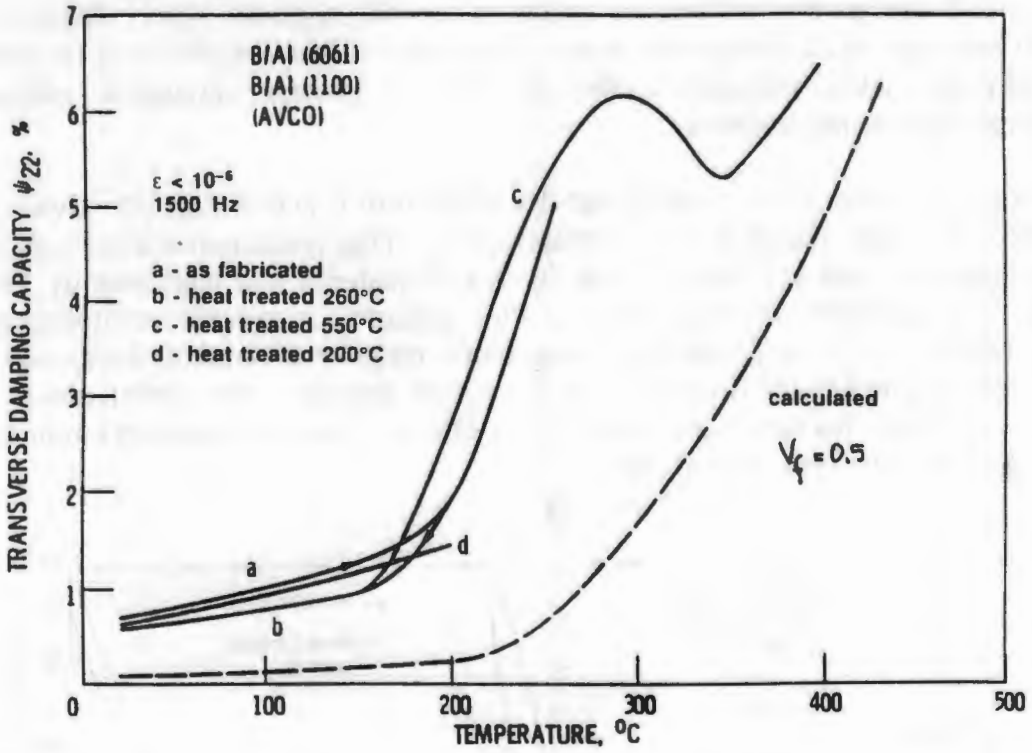

Figure 11 Transverse Damping of B/1100 Al and B/6061 Al. Curves a to c are for B/6061 Al and curve d is for B/1100 Al [23].

The transverse damping capacity of B/1100 Al and B/6061 Al are shown in Figure 11. The figure shows the results of various heat treatments, which do not appear to affect the damping capacity. The calculated transverse damping capacity of B/6061 Al with a fiber volume fraction of 0.5 is shown as a dashed line. The difference in the maximum and the minimum of the damping capacity exhibited by curve c amounts to only 15 percent.

Figure 12 summarizes the specific damping capacity of MMCs discussed above, as a function of temperature. The dark heavy line is the damping capacity of pure aluminum shown for reference. The dashes represent the damping capacity of fibers alone. This shows the strong anelastic effect on the damping capacity of boron and Borsic fibers compared to SiC fibers shown near the bottom of the graph. The difference in the damping capacity between these two types of fibers is approximately a factor of 20-30 at about 600°C. Enhancement in damping capacity of pitch-base carbon fiber has been reported elsewhere [21], and has not been added to Figure 12. The relatively large damping capacity of boron fiber is responsible for the observed large damping capacity of boron-aluminum composites. Note the low damping capacity, less than 1 percent, of Gr/Mg and SiC_f/Ti composites, while that of B/6061 Al is almost as high as the boron fiber itself.

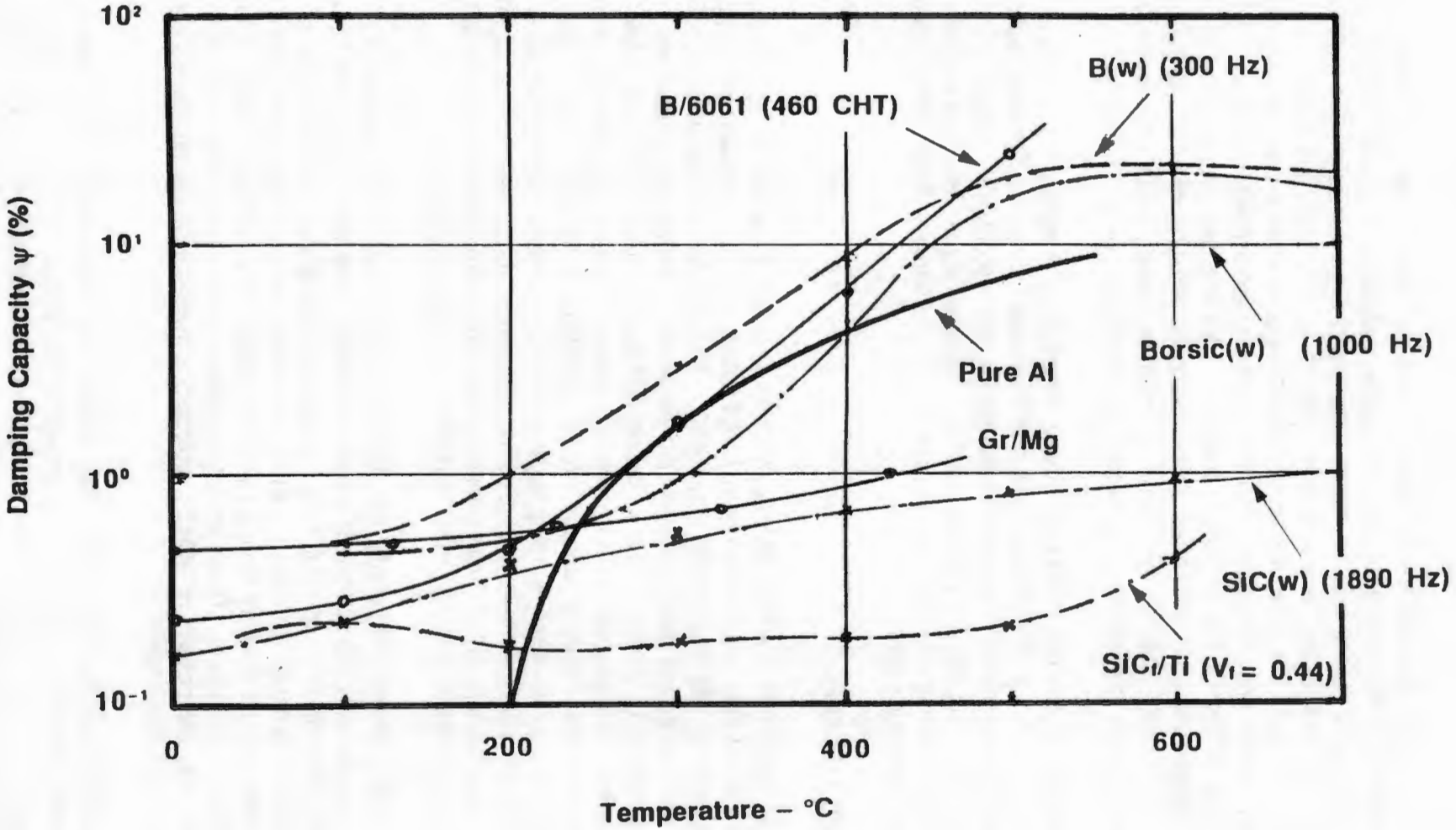

Figure 12 Summary of the Specific Damping Capacity of Some MMCs as a Function of Temperature.

Figure 13 presents a summary of specific damping capacity as a function of strain amplitude of the MMCs previously discussed. The damping capacity of pure aluminum is shown for reference. The short dashed lines represent computational predictions made with various models [5] for Gr/Mg and Gr/Al. Some of these computations included the effects of residual stresses resulting both from the difference in the coefficient of thermal expansion between fiber and matrix, and from the fiber anisotropy. Although some of these predictions agree well with measurements, that of the Gr/Mg composite does not. All the data presented in Figures 1 through 11 are represented as cross-hatched areas. Note the behavior of P55Gr/Mg - 1 at. % Mn. The damping capacity exhibits the kind of rise with increasing strain amplitude exhibited by pure aluminum, but at approximately 1.5 orders of magnitude lower strain amplitude.

A comparison of the loss factors of various materials and metal matrix composites is shown in Figure 14. Two conclusions are obvious from this figure: the damping capacity of MMCs is not better than conventional unreinforced metals, and viscoelastic materials exhibit the greatest damping. This suggests that for a material to simultaneously achieve high stiffness, high strength, and high damping capacity, the matrial should combine MMCs with viscoelastic materials. This is nothing new!

GENERAL CONCLUSIONS

As already mentioned, the most striking observation is that the damping capacity of metal matrix composites is not very good, certainly no better than unreinforced metals, except perhaps at elevated temperatures and high strain amplitudes. Dislocation substructures surrounding reinforcements tend to impart strain independent behavior to reinforced aluminum. From preliminary work reported elsewhere [21], it appears that the damping capacity of carbon-fiber-reinforced metals may be improved, but at present it remains in doubt that such improvements would raise the composite damping capacity much beyond unreinforced metals. MMCs do exhibit a somewhat equal or better damping capacity than low atomic number alloys, such as aluminum or titanium, making MMCs attractive for space structures. Nonetheless, significant increases in the damping capacity of dimensionally critical space structures must be obtained by other methods as is discussed by some other papers in these proceedings.

An important problem in assessing the state of art is the database; at present it is small and this author is unaware of any systematic efforts to compile these data. Thus, one finds ones self in the ironic situation of needing a larger database to understand the potential of these materials with regards to damping capacity. At the same time the great expectation that MMCs would exhibit high damping capacity having failed to materialize resulted in funding reduction to study these material properties. If any recommendation is to be made it is that fundamental work in understanding the physics of MMCs subjected to time-varying loads should continue with carefully planned experiments.

The theoretical analysis and model development for describing and predicting the intrinsic (or internal) damping behavior of MMCs is at present rather primitive. There are a number of microscopic models [5] used to explain and even predict performance, but they exhibit poor reliability when fiber and matrix material properties are changed. Model calculations in B/Al,

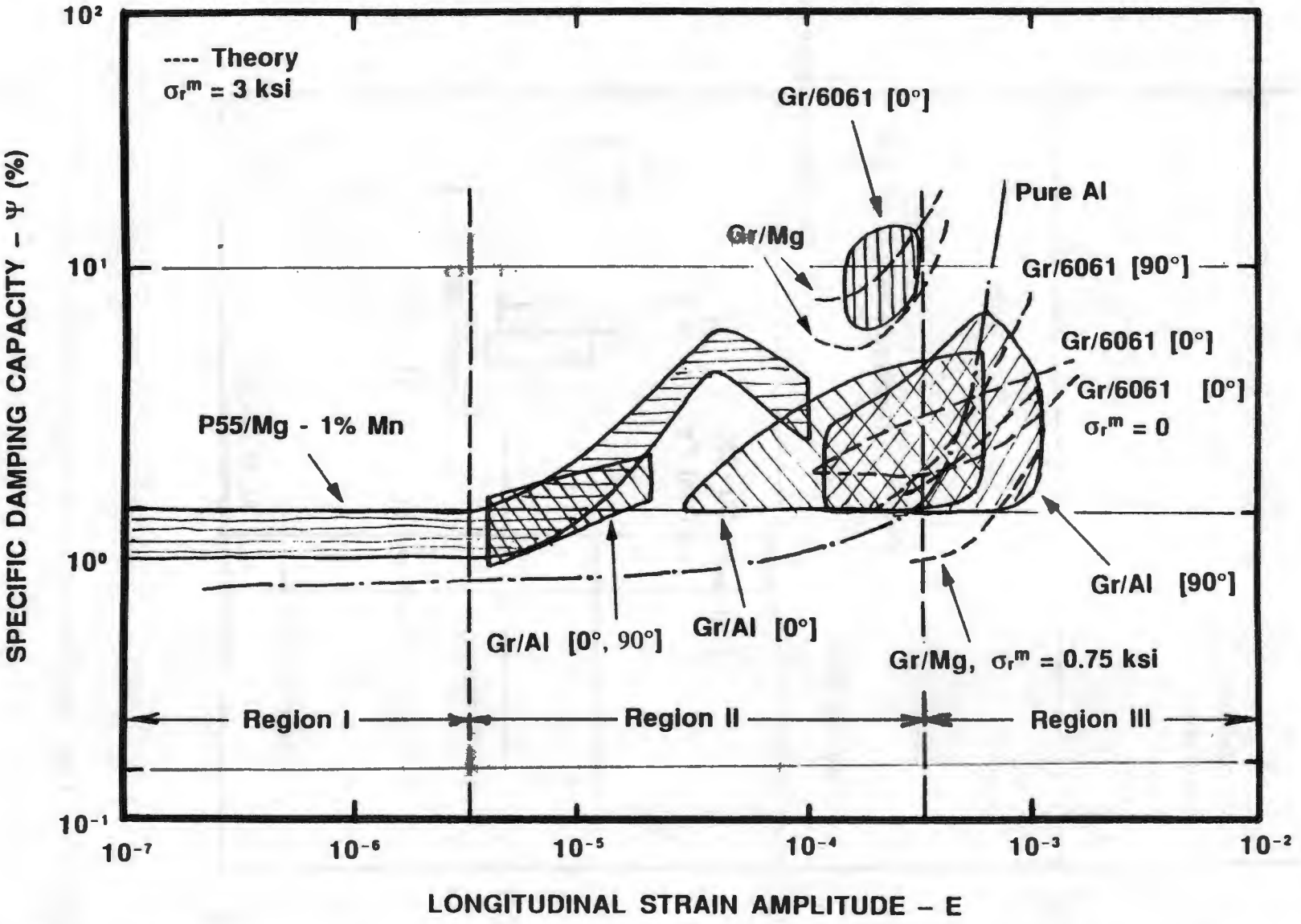

Figure 13 Summary of Specific Damping Capacity of Some MMCs as a Function of Strain Amplitude.

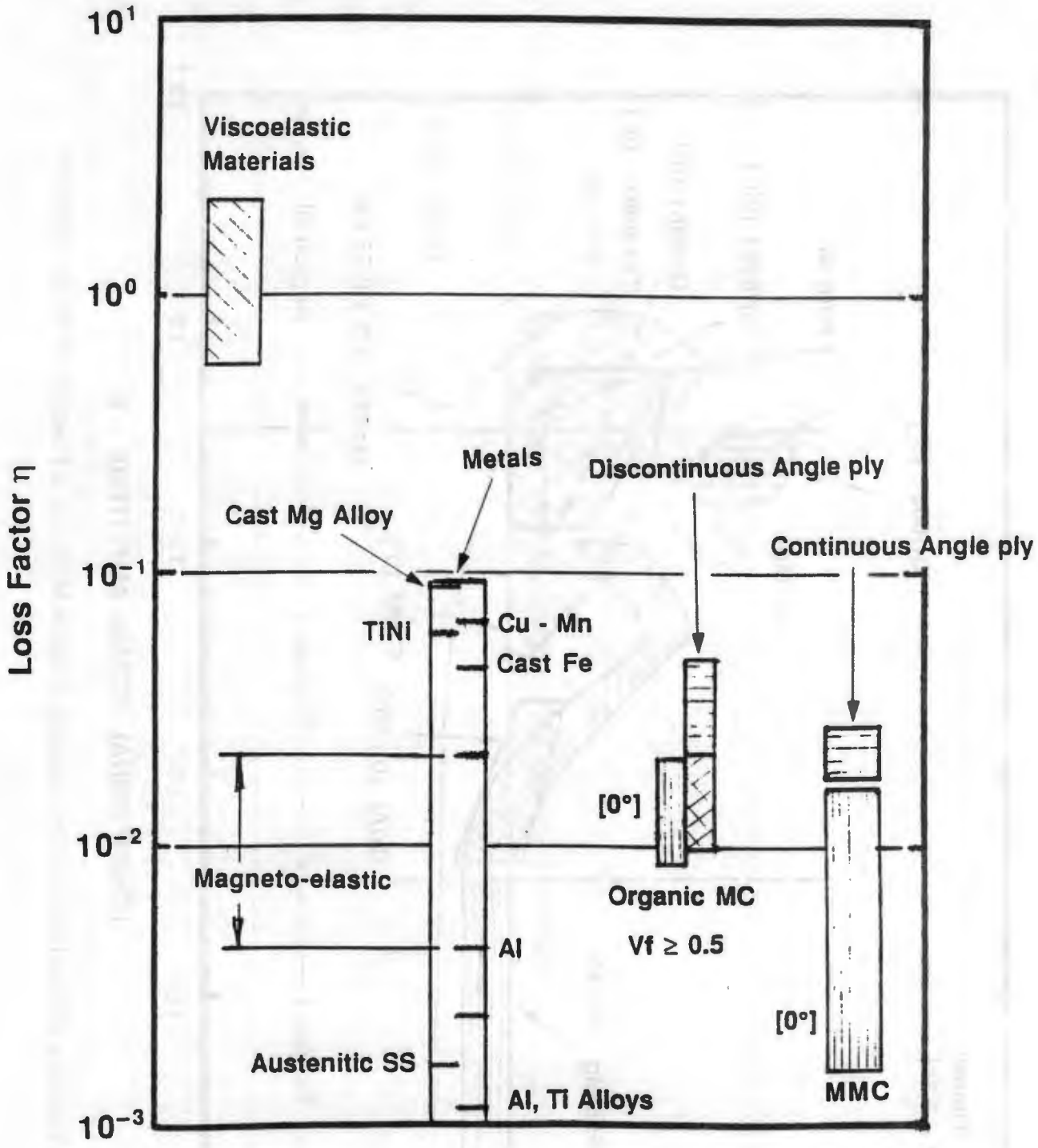

Figure 14 Loss Factor Comparisons for Various Materials [2].

for example, have predicted damping capacity values much lower than observed, implying a lack of fundamental understanding of the damping mechanisms of these complex advanced materials. Modeling of fiber damping has been fairly well developed in the Soviet Union relative to the US, but even this modeling is not enough. Theoretical analysis must consider the fiber as a composite consisting of a core (tungsten or carbon or something else) surrounded by the fiber material with an outer surface of a reaction barrier coating and/or a compliant coating. The analytical machinery is well developed and there are numerous papers available describing the application of linear elastic theory to cylindrical problems of this type. To set the stage for systematic theoretical analysis and model development, a review of theoretical work in this area should be carried out so others, including newcomers, would have a sensible place to start for developing new ideas and approaches. Any new developments in the theoretical analysis of the damping capacity of MMCs must include the phenomenology of the interface.

It is obvious from the small amount of data presented in this paper that boron fibers exhibit high damping capacity and appear to dominate the damping capacity in aluminum reinforced with boron. The SiC coating on these fibers appears to decrease the damping capacity slightly. Damping capacity of boron fibers is distinctly superior to that of SiC fibers. Damping capacity of other fibers of interest (Al_2O_3, TiB_2, B_4C coated boron), with the possible exception of carbon fibers [21], seems not to have received attention. Silicon carbide fiber on a tungsten core has a damping capacity well below boron fibers, by as much as a factor of 20-30.

Observations of the small database available indicates that the damping capacity of MMCs appears to be dependent on process method, fiber content, frequency, temperature, heat treatment, and strain amplitude. Strain amplitude in a certain range of values (10^{-5} - 10^{-3}) has a strong effect on damping capacity. This is generally believed to be due to the Zener relaxation effect, and dislocation structures can be explained to some extent by means of the Granato-Lucke theory.

Heat treatment has an effect on damping capacity in a way that is not understood. Theoretical understanding in this case appears difficult and testing various hypotheses could prove very expensive as large numbers of specimens would need to be tested and microscopically examined. Nevertheless, present observations of the effects of heat treatment on damping indicate that heat treatment decreases damping in fibers and aluminum, but increases it in carbon-fiber-reinforced magnesium.

"Someday all will be well" is our hope

"All is well today" is illusion

Voltaire, 1722.

References

1. R.L. Sheen, Experimental Measurements of Material Damping for Space Structures in Simulated Zero-G, M.S. Thesis, MIT, December 1983.

2. S.P. Rawal, T.H. Armstrong, and M.S. Misra, Interfaces and Damping in Metal Matrix Composites, Final Report, Martin Marietta Denver Aerospace, Denver, Co, December 1986

3. M.S. Misra, S.P. Rawal, and J.H. Armstrong, Damping Characteristics in Metal Matrix Composites, Technical Report, Martin Marietta Denver Aerospace, Denver, Co, November

4. J.E. Schoutens, Internal Damping in Metal Matrix Composites, MMCIAC, Kaman Sciences Corp., Santa Barbara, CA 93102, Rept. No. 720, 1990

5. A. Wolfenden and T.M. Wolla, Dynamical Mechanical Properties, in Metal Matrix Composites: Mechanisms and Properties, R. K. Everett and R. J. Arsenault, Eds., Academic Press, New York, 1991, p.287.

6. C. Zener, Phys. Rev., 60 (1941) p.906.

7. A.S. Nowick and B.S. Berry, Anelastic Relaxation in Crystalline Solids, Academic Press, New York, 1972.

8. H.M. Ledbetter, M. Lei, and M.W. Austin, Young Modulus and Internal friction of a Fiber-Reinforced composite, J. Appl. Phys., 59(6) (1986)p.1972.

9. J. DiCarlo and W. Williams, Dynamic Modulus and Damping of Boron, Silicon Carbide, and Alumina Fibers, Ceramic Engineering and Science Proceedings, Vol. 1 (1980) p.671.

10. G.N. Dugladze, G.Sh. Darsavelidze, and G.V. Tsagareishivli, High-Temperature Internal Friction in Boron Fibers, Soobsch. Akad. Nank Gruz, SSR, 70 (1) (1973) p.141.

11. G.Sh. Darsavelidze, et al., Temperature Dependence of the Internal Friction of Coated Boron Whiskers, Goobshck. Akad. Nank Gruz, 89(2) (1978) p.421.

12. G.V. Tragareishivli, et al., Internal Friction in Boron Whiskers, Boron-Production, Structures, and Properties, Nanka, Moscow, 1974.

13. V.S. Postnikov, et al., Mechanism of Absorption of Elastic Energy in Boron Fibers, Soviet Powder Metallurgy and Metal Ceramics, 22, no. 9 (249), September 1983, p.773.

14. J.E. Schoutens, Review of Some Recent Developments in the Physics of Metal Matrix Composite Materials, MMCIAC Report no. 803, 1990.

15. D.J. Nelson and J.W. Hancock, J. Mater. Sci., 13 (1978) p.2429.

16. N.N. Kishore et al., J. Reinf. Plas. Comp., 1 (1982) p.40.

17. N.N. Kishore et al., J. Reinf. Plas. Comp., 1 (1982) p.64.

18. H. M. Ledbetter and S.K. Datta, Vibration Damping Workshop 1984, AFWAL-TR-84, pp.W1-W8, Wright Patterson AFB, OH, 1984.

19. S.I. Hwang and R.F. Gibson, J. Eng. Mater. and Tech., 109 (1987) p47.

20. Z. Hashin, Trans. ASME, 32 (1965) p.630.

21. A.J. Eckel and Steven P. Jones, Controlling the Damping Behavior of Pitch-Based Carbon Fibers, these Proceedings.

22. M.S. Misra, Damping Characteristics of Metal Matrix Ccomposites, Letter Report, Martin Marietta, Denver, CO, Report no. MCR-85-721, Issue 9, 1988.

23. J.A. DiCarlo and J.E. Maisel, High Temperature Dynamic Modulus and Damping of Aluminum and Titanium Matrix Composites, NASA TM 79080, 1980.

24. F.D. Ross and L. Rubin, Acoustic Attenuation of Metal Matrix Composites, The Aerospace Corporation, Report no. SD-TR-82-62 (MMC 701706), August 1982.

25. M.S. Misra and P.D. LaGreca, Damping Behavior of Metal Matrix Composites, Martin Marietta, Denver, CO, DTIC no. ADP004704.